

Superconducting cascade electron refrigerator

M. Camarasa-Gómez,¹ A. Di Marco,² F. W. J. Hekking,² C. B. Winkelmann,^{3,4} H. Courtois,^{3,4} and F. Giazotto¹

¹NEST, Istituto Nanoscienze-CNR and Scuola Normale Superiore, I-56127 Pisa, Italy

²LPMMC-CNRS, Université Joseph Fourier, 25 Avenue des Martyrs, 38042 Grenoble, France

³Univ. Grenoble Alpes, Institut Néel, F-38042 Grenoble, France

⁴CNRS, Institut Néel, F-38042 Grenoble, France

(Dated: 15 July 2021)

The design and operation of an electronic cooler based on a combination of superconducting tunnel junctions is described. The cascade extraction of hot-quasiparticles, which stems from the energy gaps of two different superconductors, allows for a normal metal to be cooled down to about 100 mK starting from a bath temperature of 0.5 K. We discuss the practical implementation, potential performance and limitations of such a device.

Electronic heat transport at the mesoscopic scale has been in the spotlight during the last few years.¹ In particular, efforts have been made to develop different types of solid-state electronic refrigerators based on tunnel junctions between a normal metal and superconductors.² Since the first observation of electronic cooling,³ different kinds of devices have been studied such as SINIS and $S_2IS_1IS_2$, where S_1 and S_2 are different superconductors, N is a normal metal and I stands for a tunnel barrier. Symmetric structures avoid the use of any other contact than the cooling junctions, while the cooling power, being an even function of the voltage, is doubled. In every case, electronic cooling is obtained by applying a voltage bias related to the gaps of the superconductors $S_{1,2}$. This allows the extraction of hot quasiparticles from N to S_1 or from S_1 to S_2 in a SINIS or a $S_2IS_1IS_2$ structure respectively, so that as a whole cooling occurs in the normal metal or the low-gap superconductor. Such devices are of wide interest for cooling microscopic⁵ as well as macroscopic objects.⁶

In the SINIS case, the cooling power is maximum at a temperature around $T_c/3$, where T_c is the superconducting critical temperature. By exploiting aluminum (Al) as superconducting material with a critical temperature of about 1 K, this optimum occurs at a bath temperature of about 300 mK, and electronic cooling down to below 100 mK of a, for instance copper (Cu), island can be routinely achieved.² The cooling of a superconductor by quasiparticle tunneling in a $S_2IS_1IS_2$ has also been demonstrated using aluminum-oxide-titanium junctions.⁷ Operation over a wider temperature range calls for the use of alternative superconducting materials and/or new architectures. For instance, a SIS'IS nanorefrigerator based on vanadium (V) with a critical temperature of about ~ 4 K was used to efficiently cool down electrons in an Al island from 1 K to 0.4 K.⁴

In this Letter, we theoretically discuss the feasibility and performance of a multistage superconducting refrigerator, hereafter called *cascade cooler*. By using suitable materials and device parameters, we show that it is possible to cool down a normal metal with improved performance with respect to more conventional SINIS refrigerators.

We consider an electron cooler based on tunnel junctions arranged in a symmetric configuration, i.e. $S_2IS_1INIS_1IS_2$, as displayed in Fig. 1(a). The structure includes two superconductors S_1 and S_2 with respective energy gaps $\Delta_{1,2}$ so that $\Delta_1 < \Delta_2$. R_1 and R_2 denote the normal-state resistances of

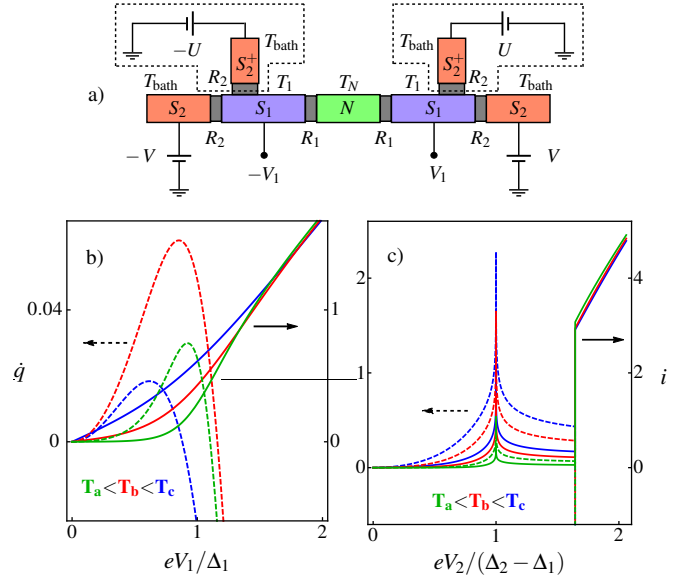


FIG. 1. (a) $S_2IS_1INIS_1IS_2$ cascade cooler geometry. The optional elements contained into the two dashed boxes enable to reach precisely the optimum bias in both the NIS_1 and the S_2IS_1 junctions. (b,c) Calculated dimensionless charge current $i = eR_{1,2}I_{N1,12}/\Delta_1$ (solid lines; right axis) and cooling power $\dot{q} = e^2R_{1,2}\dot{Q}_{N1,12}/\Delta_1^2$ (dashed lines; left axis) of a NIS_1 and a S_2IS_1 tunnel junction as a function of the dimensionless applied bias voltage eV_1/Δ_1 and $eV_2/(\Delta_2 - \Delta_1)$ for different values of T_{bath} . In (b) we set $k_B T/\Delta_1 = 0.129, 0.259, 0.474$, respectively for T_a, T_b, T_c , corresponding to temperatures 0.3, 0.6, 1.1 K in the case of Al with $\Delta_1 = 200 \mu\text{eV}$. In (c) we use 0.345, 0.560 and 0.689, corresponding to 0.8, 1.3 and 1.6 K. The ratio Δ_2/Δ_1 of 4.105 corresponds to the V-Al combination.

the individual S_1IN and S_2IS_1 junctions, respectively. The present structure actually consists of a SINIS micro-cooler to which one superconducting tunnel contact has been added at each end. In the following, the cascade cooler S_2 electrodes are voltage-biased at a voltage $\pm V$, so that the inner superconducting islands (S_1) reach a voltage $\pm V_1$. Here, we also assume that inelastic electron-electron interaction drives each individual part of the system into a quasi-equilibrium regime. Therefore, the electron populations in N and S_1 can be respectively described by a Fermi-Dirac energy distribution function at temperatures T_N and T_1 , which can largely differ

from the bath temperature T_{bath} . The outer superconductor S_2 is considered at thermal equilibrium with the phonon bath so that $T_2 = T_{bath}$.

We first discuss the behavior of each individual junction in the cascade cooler. The charge current I_{N1} and the heat current \dot{Q}_{N1} flowing from N to S_1 through a NIS_1 junction under voltage bias V_1 are given by¹

$$I_{N1} = \frac{1}{eR_1} \int_{-\infty}^{\infty} dEn_1(E - eV_1)[f_N(E) - f_1(E - eV_1)], \quad (1)$$

$$\dot{Q}_{N1} = \frac{1}{e^2R_1} \int_{-\infty}^{\infty} EdEn_1(E - eV_1)[f_N(E) - f_1(E - eV_1)] \quad (2)$$

Here, $f_{1,2,N}$ is the quasiparticle energy distribution function in S_1 , S_2 or N, respectively, and $n_{1,2}$ denotes the dimensionless BCS density of states of $S_{1,2}$ smeared by the Dynes parameter⁸ $\gamma_{1,2}\Delta_{1,2}$.

In a NIS_1 junction, a non-zero Dynes parameter for S_1 induces heating in N, so that cooling vanishes at an electron temperature $T_N \simeq T_c 2.5\gamma_1^{2/3}$. In practice, the Dynes parameter ranges from $10^{-2}\Delta_{1,2}$ to $10^{-7}\Delta_{1,2}$.¹¹ Figure 1(b) shows the voltage bias dependence of the charge and heat currents in a NIS_1 junction. At a sub-gap bias, the heat current \dot{Q}_{N1} is positive, meaning heat removal from N into S_1 . At low temperature $k_B T_N < \Delta_1$, the maximum cooling power is obtained at a voltage $eV_1 \simeq \Delta - 0.66k_B T_N$.² At this optimum value, the corresponding charge current reads

$$I_{N1,opt} \approx 0.48 \frac{\sqrt{k_B T_N \Delta_1}}{eR_1}. \quad (3)$$

As every tunneling event removes an energy of about $k_B T$, the related heat current \dot{Q}_{N1} is about $I_{N1,opt} k_B T_e / e$. For $eV_1 > \Delta_1$, the N electrode is heated with a power $-\dot{Q}_{N1}$ close to $IV_1/2$. In every case, the superconductor receives a heat $-\dot{Q}_{1N} = IV_1 + \dot{Q}_{N1} > 0$.

In a S_2IS_1 junction biased with a voltage V_2 , the charge current I_{12} and heat current \dot{Q}_{12} flowing from S_1 to S_2 are given by^{7,9,10}

$$I_{12} = \frac{1}{eR_2} \int_{-\infty}^{\infty} dEn_1(E)n_2(E - eV_2) \times [f_2(E - eV_2) - f_1(E)], \quad (4)$$

$$\dot{Q}_{12} = \frac{1}{e^2R_2} \int_{-\infty}^{\infty} EdEn_1(E)n_2(E - eV_2) \times [f_1(E) - f_2(E - eV_2)]. \quad (5)$$

Figure 1(c) shows the voltage bias dependence of the charge and heat current in S_2IS_1 case. We note the sharp maximum of thermal and charge currents occurring at a voltage bias V_2 equal to $(\Delta_2 - \Delta_1)/e$. This peak shows up only at non-zero temperatures and corresponds to electrons occupying states above the gap in S_1 tunneling to empty states below the gap in S_2 . Both the charge and the heat current at the peak are strongly affected by the temperature and the Dynes parameter. In particular, we have calculated the charge current to be

$$I_{12,opt} \approx \frac{-\sqrt{\Delta_1 \Delta_2}}{eR_2} \exp\left[-\frac{\Delta_1}{k_B T_1}\right] \ln(\sqrt{\gamma_1} + \sqrt{\gamma_2}) \quad (6)$$

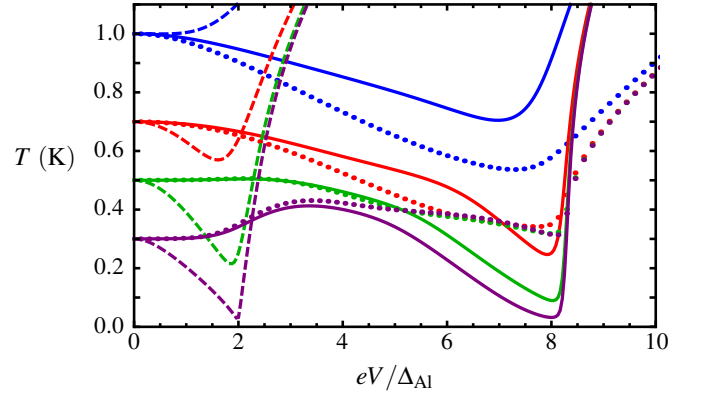


FIG. 2. Calculated temperature of the normal metal T_N (solid line) and of the superconductor S_1 T_1 (dotted lines) for a V-Al-Cu cascade cooler and for an Al-Cu SINIS refrigerator (dashed lines) as a function of eV/Δ_{Al} , at a bath temperature $T_{bath} = 1$ K (blue curves), 0.7 K (red), 0.5 K (green), and 0.3 K (purple). The parameters are $\gamma_{1,2} = 10^{-5}$, $R_1 = 500 \Omega$, $R_1/R_2 = 100$, $V_1 = V_N = 10^{-2} \mu\text{m}^3$, $\Delta_{Al} = 200 \mu\text{eV}$, $\Delta_V = 820 \mu\text{eV}$, $\Sigma_{Al} = 0.2 \times 10^9 \text{Wm}^{-3}\text{K}^{-5}$ and $\Sigma_{Cu} = 2 \times 10^9 \text{Wm}^{-3}\text{K}^{-5}$.

when $\Delta_2/\Delta_1 > T_{bath}/T_1 W > 1$. It is worth emphasizing that $I_{12,opt}$ depends logarithmically on γ_1 and γ_2 . Compared to the NIS case, the charge current is smaller by a factor of about $\exp(-\Delta_1/k_B T_1)$. The related heat current is about $I_{12,opt} \Delta_1 / e$, meaning that every tunneling event removes a heat Δ_1 from S_1 .

In a normal metal, electrons exchange heat with lattice phonons with a power¹² $P_{e-ph}(T_N, T_{bath}) = \Sigma V_N (T_N^5 - T_{bath}^5)$, where V_N is the N metal volume and Σ is the material-dependent electron-phonon coupling constant. In a superconductor, the energy gap around the Fermi level suppresses the efficiency of the electron-phonon coupling. At $T_{bath} \ll T_1 \ll \Delta/k_B$, one obtains that the power exchanged between electrons and phonons (P_{e-ph}^S) is reduced by a factor of $0.98 \exp(-\Delta/k_B T_1)$ with respect to that of the normal state.¹³

We now consider the whole cascade superconducting refrigerator. In the series configuration that we first consider, the charge currents flowing through all junctions are necessarily equal, so that

$$I_{N1} = I_{12}. \quad (7)$$

The thermal balance in N reads

$$2\dot{Q}_{N1} + P_{e-ph} = 0, \quad (8)$$

the factor 2 coming from the presence of two symmetric cooling NIS junctions. On the other hand, the thermal balance in each S_1 reads

$$\dot{Q}_{12} + \dot{Q}_{1N} + P_{e-ph}^S = 0, \quad (9)$$

where we have taken into account the heat $-\dot{Q}_{1N} > 0$ deposited by the S_1IN junction into the superconductor 1. The behavior of the cascade cooler is governed by the above three non-linear integral equations. It depends strongly on different parameters such as the dimensionless Dynes parameters

$\gamma_{1,2}$, the N and S_1 volumes $\mathcal{V}_{N,1}$, the choice of the materials, the bath temperature, and the junction resistances $R_{1,2}$. As for the latter, it is crucial that the two cooling junctions NIS_1 and S_1IS_2 reach together their optimum cooling point at a given global bias V . A first naive assumption would be to assume that the currents at the optimum bias point are close to the Ohm's law value, so that the resistance balance would read $(\Delta_2 - \Delta_1)/R_2 = \Delta_1/R_1$. This is actually incorrect, as the current through the S_2IS_1 junction is far from being Ohmic and depends strongly on the Dynes parameters.

In order to be more specific, let us consider as a first combination of materials vanadium, aluminum and copper. Based on its critical temperature of about 4 K, vanadium brings a good efficiency for electronic cooling from a bath temperature around 1 K.⁴ An aluminum island cooled in this way can reach a temperature close to the operation range of usual aluminum-based SINIS coolers. A cascade combination of V-Al₂O₃-Al and Al-Al₂O₃-Cu junctions therefore seems promising. Figure 2 compares the behavior of a Al-Cu SINIS refrigerator (dashed lines) to a V-Al-Cu cascade cooler (solid lines) with usual parameters values, a common tunnel resistance R_1 value of 500 Ω and a resistance ratio R_1/R_2 of 100, close to the optimum (see below). From Fig. 2, the electronic cooling of the N island (full lines) is more efficient in the cascade system, which performs well up to 0.7 K whereas the SINIS refrigerator (dashed lines) is little efficient. At a bath temperature of 1 K, the SIN stage is inefficient, while the SIS stage operates well. The capability of the cascade refrigeration scheme is illustrated by the large quasiparticle cooling obtained in S_1 at every bath temperature below 1 K (dotted lines).

Still in the case of a V-Al-Cu device, Figure 3 displays the minimum achieved electronic temperature in N (T_N) [panel (a)] and the voltage drops $V_{1,opt}$ and $V_{2,opt}$ [panel (b)] across the two S_1IN and S_2IS_1 junctions at the minimum temperature T_N versus the junctions' resistance ratio R_1/R_2 . A bath temperature T_{bath} of 0.5 K and a fixed resistance R_1 of 500 Ω is considered here. At large R_1/R_2 value, the S_1IN junctions dominate and the optimum cooling is obtained at a voltage drop V_1 close to the expected value $(\Delta_1 - k_B T_N)/e$. At small R_1/R_2 value, it is the S_2IS_1 junctions that dominate, and the optimum cooling is obtained at V_2 close to the expectation $(\Delta_2 - \Delta_1)/e$. Overall, the best performance is obtained in the region where the two kinds of junctions can operate close to the optimum. Here, the parameters are $\gamma_{1,2} = 10^{-5}$ and 10^{-4} and $\mathcal{V}_N = 10^{-2} \mu\text{m}^3$. We have used the well-accepted material-specific values $\Sigma_{Al} = 0.2 \times 10^9 \text{Wm}^{-3}\text{K}^{-5}$ and $\Sigma_{Cu} = 2 \times 10^9 \text{Wm}^{-3}\text{K}^{-5}$. In this case, we achieve a good and somewhat constant performance for a resistance ratio between 10 and 200. This order of magnitude is consistent with the factor $\exp(\Delta_1/k_B T_1)$ between the currents $I_{N1,opt}$ and $I_{12,opt}$ at an identical junction resistance $R_{1,2}$. The relatively large span of this region stems from the existence of the singularity in the electric current as a function of the bias voltage. This rectifies any imbalance that might occur in the structure, similarly to what happens for an asymmetric pair of NIS junction in series.¹⁶ At higher bath temperature, the window for optimal resistance ratio gets narrower, and is slightly shifted towards lower values.

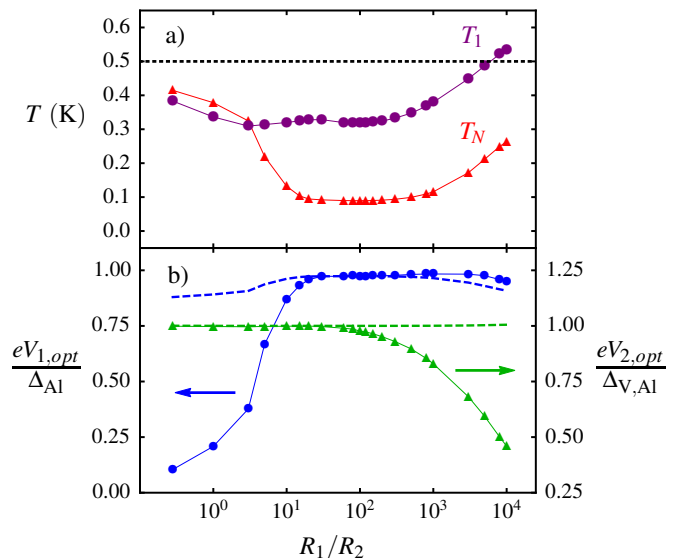


FIG. 3. (a) Calculated minimum temperature of the normal metal $T_{N,min}$ (red triangles) and the related temperature of low-gap superconductor T_1 (purple disks) of a V-Al-Cu cascade cooler at its optimum bias point as a function of the ratio R_1/R_2 for a bath temperature $T_{bath} = 0.5$ K. (b) Related dimensionless voltage drops $eV_{1,opt}/\Delta_{Al}$ (blue; left axis) and $eV_{2,opt}/\Delta_{V,Al} = eV_{2,opt}/(\Delta_V - \Delta_{Al})$ (green; right axis) across the S_1IN and S_2IS_1 junctions, respectively, as a function of R_1/R_2 . The bath temperature considered here is 0.5 K. The other parameters are identical to the ones of Fig. 2. Also shown are the predictions $eV_{1,opt} = \Delta_1(T_1) - 0.66k_B T_N$ (dashed blue line) and $eV_{2,opt} = \Delta_2(T_{bath}) - \Delta_1(T_1)$ (dashed green line).

Let us now discuss practical issues in a cascade cooler's design. As stated above, the performance of the cascade cooler configuration strongly depends on the value of the ratio R_1/R_2 . Due to the smaller value of the current I_{12} through a S_1IS_2 junction compared to the current I_{N1} through a S_1IN junction of comparable normal-state conductance, the resistance R_2 has to be made significantly smaller than R_1 in order to get an efficient cascade cooler. Optimal values of the R_1/R_2 ratio for bath temperatures and material configurations of experimental interest therefore lie in the range $\sim 15 - 150$, while depending strongly on subtle parameters like the Dynes parameters of $S_{1,2}$. From the fabrication point of view, it might be difficult to tune the R_1/R_2 ratio at its optimum with a good degree of precision. This leads to the practical necessity of tuning the voltage V_1 independently from the the main bias voltage V . One possible solution to this problem is to tunnel-couple to each S_1 electrode an additional superconductor S'_2 , as shown in Fig. 1(a). Biasing with a second positive (negative) voltage U these two tuning junctions would enable to add (subtract) some current in the S_1IS_2 junctions compared to the S_1IN ones. The S_1INIS_1 current can then be tuned from zero to the double of its value at zero bias U . The latter limitation comes from the fact that the voltage U needs to be always sub-gap in order to prevent any extra heating of the S_1 electrode.

For practical sample fabrication issues, one would preferably use the same tunnel barrier characteristics (in particular

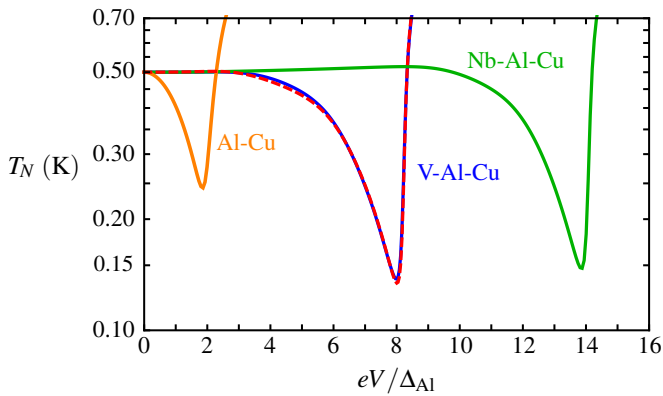


FIG. 4. Calculated normal metal temperature T_N in a cascade cooler for $T_{bath} = 0.5$ K as a function of the dimensionless bias voltage eV/Δ_{Al} , in different cases: Al-Cu one-stage cooler (orange), V-Al-Cu (dotted red) with identical volumes for N and S_1 , V-Al-Cu (blue) and Nb-Al-Cu (green) with volumes adapted to the resistances' ratio so that $\mathcal{V}_1/\mathcal{V}_N = R_1/2R_2$. The ratio R_1/R_2 is set at the optimal value in every case: 100 (V-Al-Cu), 30 (Nb-Al-Cu), 80 (V-Al-Cu, adapted volumes' ratio) respectively. We take $\Delta_{Nb} = 1407 \mu\text{eV}$, $R_1 = 1 \text{ k}\Omega$. The other parameters are identical to Fig. 2, including $\mathcal{V}_N = 10^{-2} \mu\text{m}^3$.

transparency) for the two tunnel barriers between S_1 on one side, and N or S_2 on the other side. Sticking to a particular value of the tunnel resistance ratio, and using similar thicknesses for N and S_1 , thus leads to a volume ratio $\mathcal{V}_1/\mathcal{V}_N$ between the superconductor S_1 and the normal metal N approximately equal to half the inverse of the resistance ratio R_1/R_2 . Furthermore, the values of the two superconductors' gaps can also be varied, for instance replacing vanadium with niobium (Nb). Figure 4 shows the results for the electron temperature T_N obtained with the two materials choices V-Al-Cu, Nb-Al-Cu, at $T_{bath} = 0.5$ K, relating or not the volumes' ratio to the resistances' ratio. The optimum resistance ratios were adjusted in every case, to respectively 30 for Nb-Al-Cu, 80 for V-Al-Cu when the volume ratio is adapted to the resistance ratio, 100 for V-Al-Cu with identical volumes \mathcal{V}_1 and \mathcal{V}_N . Imposing a larger volume \mathcal{V}_1 affects only slightly the performance of the whole device, with a minimum electronic temperature rising from 134 to 138 mK for the V-Al-Cu material combination. This value increases to 147 mK when V is replaced by Nb. A larger gap value does not necessarily provide an improved cooling, because it also reduces the available heat current in the S_1IS_2 junction.

Another crucial issue for the present cascade electronic cooler resides in a proper quasiparticle thermalization in the intermediate superconductor S_1 . It is well known that superconducting-based electronic refrigerators generally suffer from poor evacuation of highly-energetic quasiparticles in the superconducting electrodes.¹⁷ To this end, quasiparticle traps of various kinds have been envisaged in order to allow their evacuation into nearby-connected normal metal layers.^{18,19} In the present design, the outer superconductor S_2 actually plays this role, with an increased efficiency thanks to its density of states singularity at the gap edge. An in-

complete quasiparticle energy relaxation in the superconductor S_1 should actually not hinder the cooling in the low-gap superconductor S_1 compared to the present quasi-equilibrium calculations. The cascade cooler appears as rather immune against poor electronic equilibration in S_1 . Finally, the outer superconducting electrodes S_2 can be efficiently thermalized through quasiparticles traps, just as it is done in the case of conventional superconducting refrigerators.¹

In conclusion, we have discussed a novel kind of electronic cooler based on hybrid superconducting tunnel junctions. A cascade geometry allows to cool a first superconducting stage, which is used as a local thermal bath in a second stage. The correct operation of the device strongly depends on the matching between the resistances of the two kinds of tunnel junctions. The resulting constraint can be easily implemented in a practical device, using of a set of two additional tunnel junctions. Decoupling of local phonon population from the thermal bath¹⁴ in a suspended metal geometry¹⁵ would improve performances compared to the situation considered here.

We acknowledge the Marie Curie Initial Training Action Q-NET no. 264034 and the EU Capacities MICROKELVIN project no. 228464 for partial financial support. We thank L. M. A. Pascal for her contribution at the very beginning of this project, A. Ronzani for help in numerics, and J. P. Pekola for fruitful discussions.

- ¹F. Giazotto, T. T. Heikkilä, A. Luukanen, A. M. Savin, and J. P. Pekola, *Rev. Mod. Phys.* **78**, 217 (2006).
- ²J. T. Muhonen, M. Meschke, and J. P. Pekola, *Rep. Prog. Phys.* **75**, 046501 (2012).
- ³M. Nahum, T. M. Eiles and J. M. Martinis, *Appl. Phys. Lett.* **65**, 3123 (1994).
- ⁴O. Quaranta, P. Spathis, F. Beltram, and F. Giazotto, *Appl. Phys. Lett.* **98**, 032501 (2011).
- ⁵A. M. Clark, N. A. Miller, A. Williams, S. T. Ruggiero, G. C. Hilton, L. R. Vale, J. A. Beall, K. D. Irwin, and J. N. Ullom, *Appl. Phys. Lett.* **86**, 173508 (2005).
- ⁶P. J. Lowell, G. C. O'Neil, J. M. Underwood, and J. N. Ullom, *Appl. Phys. Lett.* **102**, 082601 (2013).
- ⁷A. J. Manninen, J. K. Suoknuuti, M. M. Leivo, and J. P. Pekola, *Appl. Phys. Lett.* **74**, 3020 (1999).
- ⁸R. C. Dynes, J. P. Garno, G. B. Hertel, T. P. Orlando, *Phys. Rev. Lett.* **53**, 2437 (1984).
- ⁹B. Frank and W. Krech, *Phys. Lett. A* **235**, 281 (1997).
- ¹⁰F. Giazotto and J. P. Pekola, *J. Appl. Phys.* **97**, 023908 (2005).
- ¹¹J. P. Pekola, V. F. Maisi, S. Kafanov, N. Chekurov, A. Kempinen, Yu. A. Pashkin, O.-P. Saira, M. Möttönen, and J. S. Tsai, *Phys. Rev. Lett.* **105**, 026803 (2010).
- ¹²F. C. Wellstood, C. Urbina, and J. Clarke, *Phys. Rev. B* **49**, 5942 (1994).
- ¹³A. V. Timofeev, C. Pascual Garcia, N. B. Kopnin, A. M. Savin, M. Meschke, F. Giazotto, and J. P. Pekola, *Phys. Rev. Lett.* **102**, 017003 (2009).
- ¹⁴L. M. A. Pascal, A. Fay, C. B. Winkelmann, and H. Courtois, *Phys. Rev. B* **88**, 100502 (2013).
- ¹⁵H. Q. Nguyen, L. M. A. Pascal, Z. H. Peng, O. Buisson, B. Gilles, C. B. Winkelmann, and H. Courtois, *Appl. Phys. Lett.* **100**, 252602 (2012).
- ¹⁶J. P. Pekola, A. J. Manninen, M. M. Leivo, K. Arutyunov, J. K. Suoknuuti, T. I. Suppala, B. Collaudin, *Physica B* **280**, 485 (2000).
- ¹⁷S. Rajauria, H. Courtois and B. Pannetier, *Phys. Rev. B* **80** 214521 (2009), and references therein.
- ¹⁸G. C. O'Neil, P. J. Lowell, J. M. Underwood, and J. N. Ullom, *Phys. Rev. B* **85**, 134504 (2012).
- ¹⁹H. Q. Nguyen, T. Aref, V. J. Kauppila, M. Meschke, C. B. Winkelmann, H. Courtois, and J. P. Pekola, *New J. of Phys.* **15**, 085013 (2013).